

Hierarchical Carbon Nanowire Microarchitectures Made by Plasma-Assisted Pyrolysis of Photoresist

Michaël F. L. De Volder,^{†,‡,*} Rob Vansweevelt,[§] Patrick Wagner,^{†,§} Dominiek Reynaerts,[‡] Chris Van Hoof,[†] and A. John Hart[†]

[†]IMEC, Kapeldreef 75, 3001 Heverlee, Belgium, [‡]KULeuven, Celestijnenlaan 300B, 3001, Leuven, Belgium, [§]IMOMEC-IMO, Hasselt University, Wetenschapspark 1, 3590 Diepenbeek, Belgium, and [†]University of Michigan, 2350 Hayward Street, Ann Arbor, Michigan 48109, United States

Ranging from graphene sheets to fullerenes, nanotubes (CNTs), and diamond-like coatings, various types of carbon nanostructures have been developed, each with their own fascinating properties. Besides these well-known allotropes, amorphous carbon is a particularly interesting material, as it shows a wide electrochemical stability window, excellent biocompatibility, and high thermal conductivity.^{1–4} For these reasons, as well as its cost-effective fabrication, pyrolyzed carbon has found wide applications in microsystems, including heat exchangers,¹ chemical probes,⁴ lab on a chip systems,^{3,5} biosensors,^{6,7} and fuel cells,^{8,9} and it has been implanted over a million times in heart valves and orthopedic joints.¹⁰ However, relatively few methods have been developed for the fabrication of amorphous carbon nanowires (CNWs), the most common probably being pyrolysis of electrospun polymers.^{11–15} While this process is interesting for fabricating mats of randomly oriented nanowires, it does not facilitate the fabrication of high aspect ratio structures nor structures having anisotropic properties as observed in vertically aligned CNT forests.

Here we show that novel anisotropic microarchitectures comprising vertically aligned CNWs can be made by oxygen plasma treatment of a patterned photoresist, followed by pyrolysis. Interestingly, these structures can also be shaped into deterministic three-dimensional (3D) hierarchical structures where nanowires are anchored to a micro-sized solid carbon core. These structures are reminiscent of biological dendrite architectures that emerged in nature as an optimization between the maximization of a surface area and the minimization of transport losses.^{16–19} Mimicking such structures in engineering could play a key role in the development of new electrodes for

ABSTRACT We present a new approach for the fabrication and integration of vertically aligned forests of amorphous carbon nanowires (CNWs), using only standard lithography, oxygen plasma treatment, and thermal processing. The simplicity and scalability of this process, as well as the hierarchical organization of CNWs, provides a potential alternative to the use of carbon nanotubes and graphene for applications in microsystems and high surface area materials. The CNWs are highly branched at the nanoscale, and novel hierarchical microstructures with CNWs connected to a solid amorphous core are made by controlling the plasma treatment time. By multilayer processing we demonstrate deterministic joining of CNW micropillars into 3D sensing networks. Finally we show that these networks can be chemically functionalized and used for measurement of DNA binding with increased sensitivity.

KEYWORDS: carbon nanofibers · pyrolysis · amorphous carbon · biosensors · hierarchical · 3D nanostructures

microsensors,^{20,21} bioprobes,²² batteries,¹² and fuel cells,⁹ as well as for various biomimetic applications.^{18,23,24} In this paper, we show that 3D microstructures made from CNW forests can be chemically functionalized and serve as an electrically integrated biosensor, with a 40% decrease in electrical resistance upon DNA binding.

RESULTS AND DISCUSSION

The CNW fabrication process begins by patterning of SU-8 microstructures by standard UV photolithography (Figure 1A). SU-8 is a negative photoresist that is commonly used to fabricate high aspect ratio microstructures and does not reflow during pyrolysis.^{2,4} Next, the sample is exposed to a harsh O₂ plasma treatment (5–60 min, 300 W, 200 sccm O₂, 150 mTorr in an 8 in. Tempress ML 200 plasma etcher), which establishes the anisotropic nanowire texture of the SU-8 (see Figure 1B). We believe different mechanisms enable the formation of SU8 nanowires. First, SU8 photoresist contains antimony, which is accumulated

* Address correspondence to Michael.devolder@imec.be.

Received for review May 29, 2011 and accepted July 8, 2011.

Published online July 08, 2011
10.1021/nn201976d

© 2011 American Chemical Society

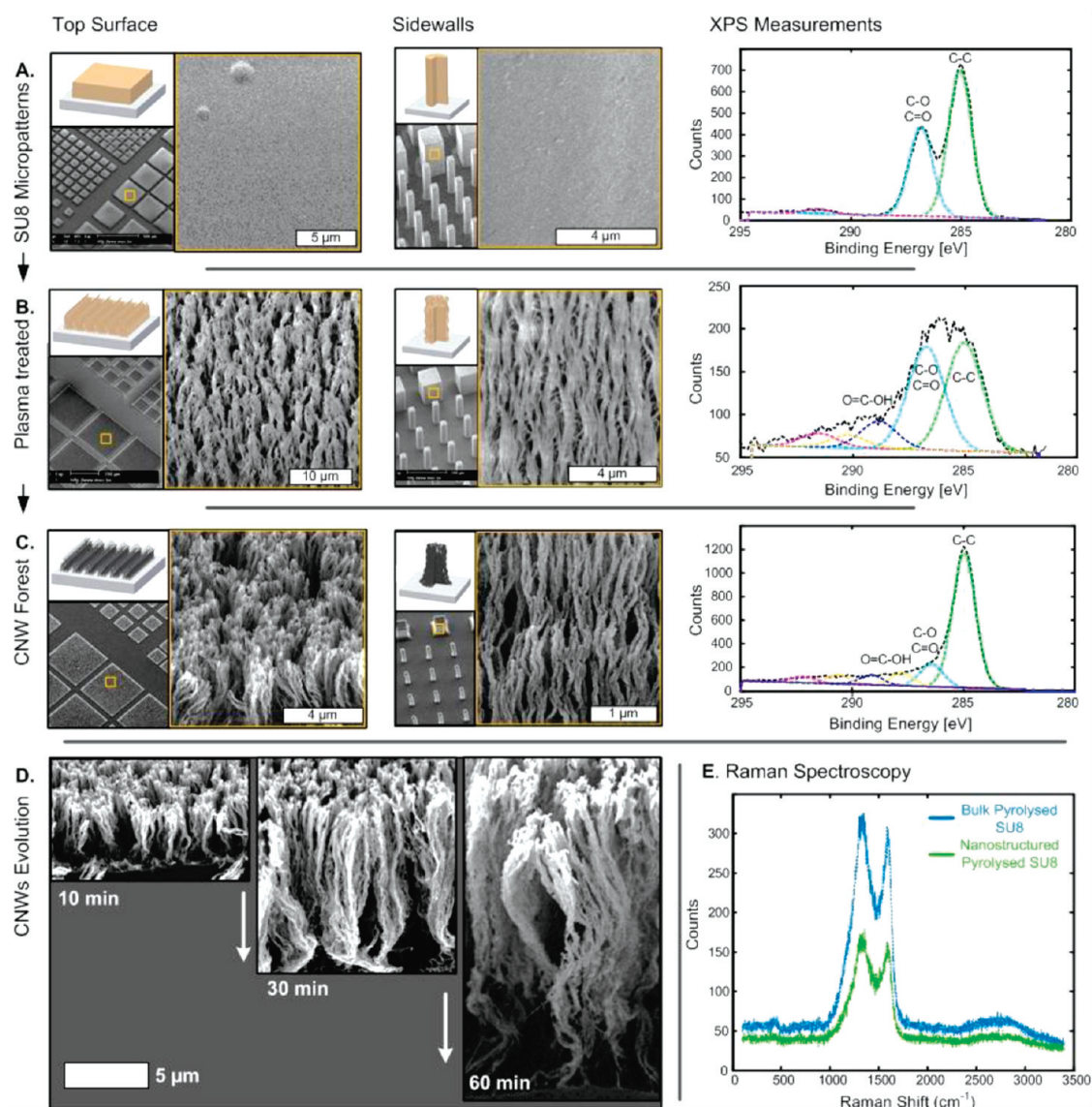


Figure 1. Illustration and SEM images of the top surface and sidewalls of CNW forests at different stages of the fabrication process, along with corresponding XPS data: SU8 pillars (A) after development, (B) after oxygen plasma, and (C) after pyrolysis. (D) Evolution of the CNW forest with increasing plasma treatment time, followed by identical pyrolysis treatment. (E) Raman spectroscopy of bulk pyrolyzed SU8 and CNWS.

at the surface upon plasma etching, and can reach up to 19% of the surface composition of our samples after plasma treatment, as observed through XPS (X-ray photoelectron spectroscopy) analysis (see Supporting Information Table S1).²⁵ Antimony, together with small amounts of aluminum that are sputtered from the plasma chamber, can locally mask the SU8 film and thereby induce the formation of nanowires.²⁶ This masking effect, combined with the directionality of the plasma treatment, induces a vertically oriented texture to the SU-8 during plasma treatment, as shown in Figure 1. Further, SU-8 mainly comprises bisphenol A-epichlorohydrin-formaldehyde copolymer (an epoxy/phenolic resin).²⁷ Therefore, the nanowire formation could be enhanced due to differences in etch rates between aromatic and linear parts of the polymer chain,

similar to surface roughening observed in polyether ether ketone as well as polyethylene terephthalate during plasma etching.^{26,28}

Interestingly, we found that these nanofilaments are maintained during pyrolysis, resulting in “forests” of vertically aligned carbon nanowires (Figure 1C). Pyrolysis was performed by heating the samples in a nitrogen environment to 300 °C (40 min ramp followed by 30 min hold) and subsequently to 900 °C (90 min ramp followed by 60 min hold) followed by a slow cooling to room temperature (at least 12 h), similar to processes reported for carbon MEMS (microelectromechanical systems).^{1,2,4,10,12,29} During pyrolysis, all volatile components evaporate from the SU8, causing shrinkage of the SU8 nanowires. The wires are initially approximately 100 nm in diameter and only 15–30 nm

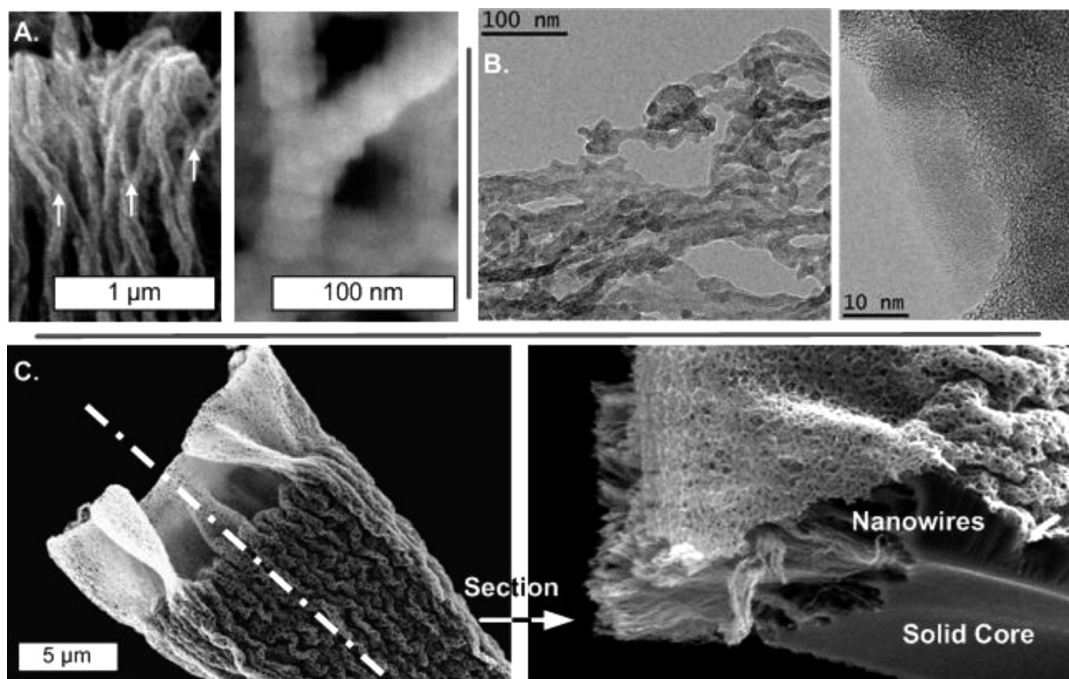


Figure 2. Details of the CNW forest morphology. (A) SEM images of aligned topology and Y-junctions (arrows) of pyrolyzed CNWs. (B) TEM image of the CNWs after pyrolysis. (C) Cross-section view of a pillar showing its hierarchical structure where the CNWs are attached to a solid core. The size of the core is controlled by the plasma treatment time.

after pyrolysis. XPS characterization shows that nearly all oxygen is removed during pyrolysis, and interestingly, no traces of antimony were detected after pyrolysis (see Table S1). The height over which the nanowires span can be simply controlled by the initial thickness of the SU8 layer and the parameters of the oxygen plasma treatment; for instance, longer plasma treatment allows etching through thicker SU8 structures. We found typical “forest” heights of 6 μm after 10 min, 13 μm after 30 min, and 27 μm after 60 min plasma treatment, as shown in Figure 1D. To our knowledge, the formation of SU-8 nanowires by plasma treatment, and their transformation into carbon nanowires, has never been shown before.

Unlike carbon nanotube forests grown by chemical vapor deposition (CVD),^{30,31} the CNW forests are highly branched (Figure 2A), and the individual wires consist of amorphous carbon (see Raman spectroscopy Figure 1E, and TEM Figure 2B). While amorphous CNWs will not match the unique mechanical and electrical properties of CNTs,³² CNWs may offer advantages in applications needing chemical functionalization^{6,7,33} or where metal catalyst particles typically used for CNT synthesis (*e.g.*, Fe, Ni, or Co) are prohibited. Further, the proposed fabrication technology is easily accessible and cost-effective, especially because the lithography step could be replaced by SU8 transfer molding.³¹ Further, by subsequently coating and developing SU8 layers³⁴ prior to plasma etching and pyrolysis, multilevel nanowire forests are made (see Figure 3A–C). By controlling the plasma time, the depth over which the

nanowires extend is changed (Figure 1D); thus structures consisting entirely of nanowires can be fabricated as well as micropillars with a solid core surrounded by a nanowire network as illustrated in Figures 2C and 3A. The relative amounts of solid and nanoporous carbon can be finely controlled by the plasma parameters, providing a straightforward means of manipulating the hierarchical structure. In these unique hierarchical structures, the core conveys mechanical robustness as well as low overall electrical resistivity, and the CNWs provide a high active surface area, which is reminiscent of natural networks and dendrites.^{16,18}

The mechanical and electrical properties of pyrolyzed carbon have been studied previously and depend on many process parameters including for instance the pyrolysis temperature. As documented by Schueller *et al.*,¹ the electrical conductivity of pyrolyzed carbon typically ranges from 1 to 100 S/cm, and the Young's modulus is 10–40 GPa. We expect comparable, if not greater, properties for CNW structures due to their anisotropic texture; however, this is the subject of ongoing work that is beyond the present scope. Nevertheless, we have verified that the adhesion of the CNW structures to the substrate is sufficient to enable subsequent lithographic postprocessing. This is illustrated in Figure 3E–H, where SU8 2050 is spincoated on top of CNW microstructures and is subsequently exposed and developed, resulting in microstructures consisting of both carbon and SU8.

Multistage processing emphasizes the ability to integrate CNW structures in microsystems and other

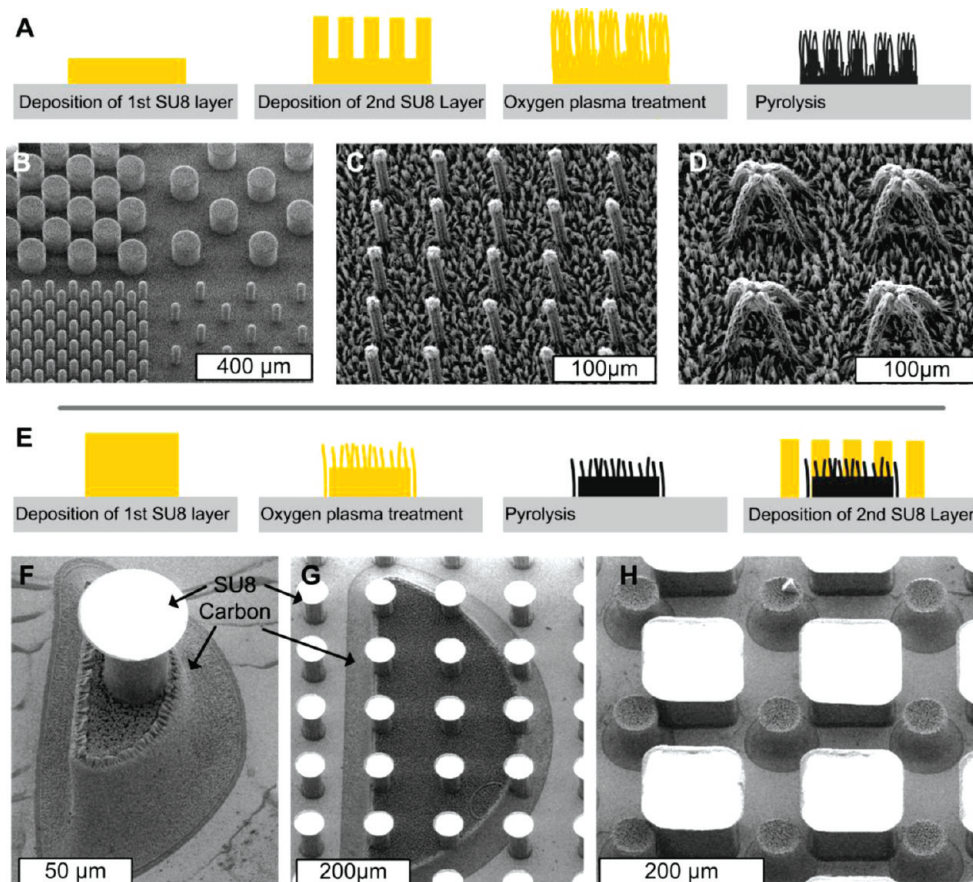


Figure 3. Examples of multilayer processing. (A) Schematic illustration of multiheight CNW structures. (B) Array of multiple height SU8 pillars after plasma treatment yet before pyrolysis. (C) Multiple height CNW array after pyrolysis. (D) Multiple height 3D CNW microstructure array after pyrolysis. (E) Schematic illustration of carbon structures with SU8. (F, G) SEM images of SU8 pillars patterned on top of hierarchical CNW structures. (H) SU8 pillars patterned in between pyrolyzed carbon hierarchical structures.

device applications; however, in general it is also necessary to interconnect microstructures in a desired and deterministic configuration. For this specific need, we have implemented a method of 3D structuring to create self-connected networks of CNW micropillars.^{2,34} First, we took advantage of the “T-topping” effect,³⁵ by forming a thin overlayer spanning adjacent SU8 microstructures (see Figure 4A). The formation of the overlayer was induced by soft-baking in convection ovens rather than on hot plates² and by exposure to a broad UV spectrum source.³⁵ As previously reported for the fabrication of suspended carbon sheets,² the formation of these films does not require a second exposure step. Second, we take advantage of the lateral shrinkage of the overlayer during pyrolysis, which pulls adjacent pillars together into three-dimensional canopies shown in Figure 4A,B. Diverse canopy shapes are fabricated in a controlled way by changing the layout of the micropillars that support the overlayer. The transformation of the SU8 structures into 3D carbon shapes can be predicted qualitatively using finite element models (FEM) where the pyrolysis is simulated as an isotropic thermal contraction problem (Comsol), as shown in Figure 4A. This 3D fashioning method can be combined

with the hierarchical nanowire network fabrication described above, by simply applying the oxygen plasma treatment before the pyrolysis (Figure 5A–D), and can also be combined with multiple-height processing (Figure 3D).

Further, CNW processing can enable the design and construction of electrically integrated 3D microarchitectures using only planar patterning operations. For this, we first define bottom electrodes made either by pyrolysis of SU8, similar to ref 2 (Figure 4C,D), or by TiN lift-off patterning (Figure 5A,C). Next, the SU8 pillars needed for the pyrolysis are defined. We found that simply changing the spacing between the pillars induces structures ranging from arches (Figure 5A,B) to extremely fine suspended bridges (Figure 5C,D). The bridges have a lateral dimension of approximately 1 μm and consist of a network of CNWs with a diameter of 30 nm or less (Figure 5D). These delicate structures are found repeatedly across arrays of micropillars (Figure 5C). In what follows, first steps to develop a DNA sensor from these electrically integrated CNW architectures are presented.

Because of its low cost, electrochemical stability, and biocompatibility, amorphous carbon is an interesting

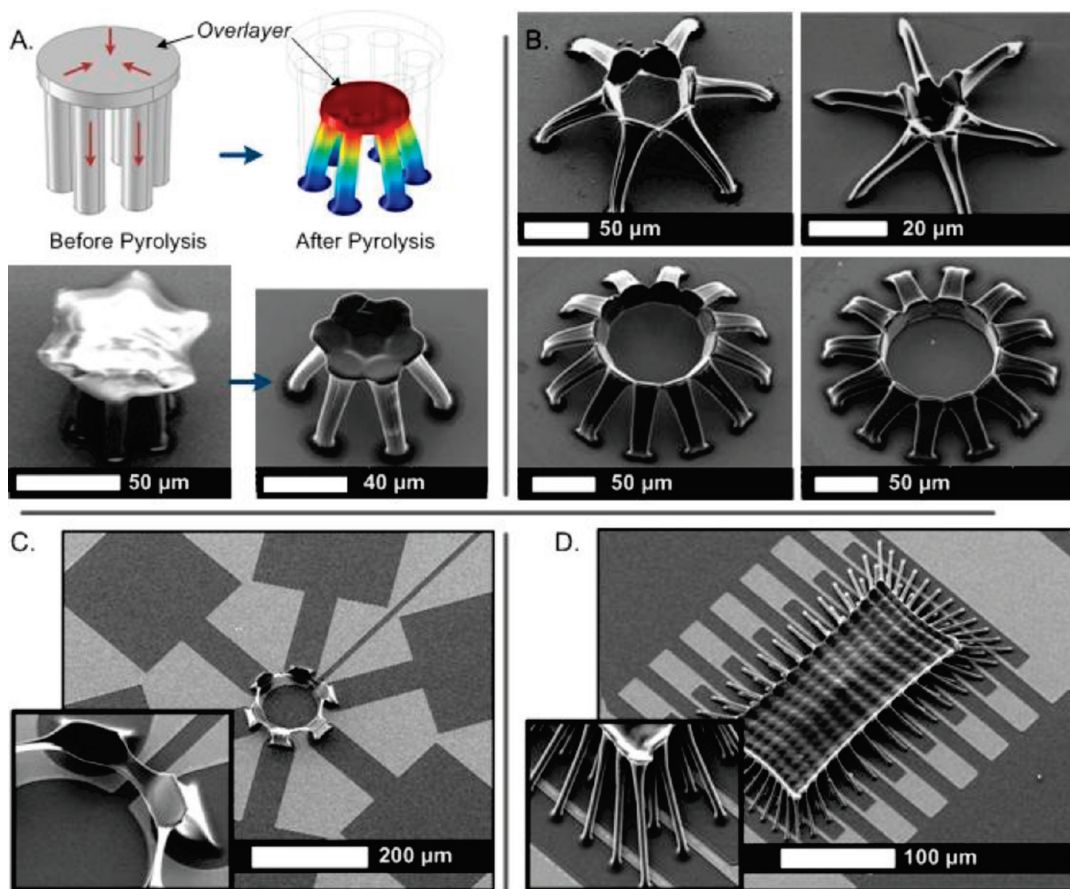


Figure 4. Examples of intricate amorphous carbon microarchitectures. (A) FEM simulation and SEM images of the 3D carbon microarchitecture formation by the directed shrinkage of an SU8 topping layer during pyrolysis. (B) SEM images of six- and 12-legged 3D geometries. Left and right images have a different tilt angle, which is controlled by the pillar height. (C) 3D circular bridge with six legs and integrated pyrolyzed carbon bottom electrodes. (D) 3D arrangement of 180 legs connecting a suspended carbon sheet to interdigitated bottom electrodes.

material for DNA biosensors.^{6,7} While existing systems are using sophisticated readout systems based on for instance quartz crystal microbalances⁷ or ac impedimetric measurements,⁶ we propose a simple resistive DNA binding detection based on the unique 3D hierarchical structures that self-connect two planar electrodes. Single-stranded DNA was covalently coupled to the carbon structures via UV photoattachment of a fatty acid linker molecule, as illustrated in Figure 5E (details provided in the SI). A similar method has been used to functionalize graphene-like flakes³⁶ and diamond-like coatings.³⁷ Confocal fluorescence microscopy images of fluorescently labeled DNA bonded to hierarchical CNWs structures (Figure 5F) as compared to pyrolyzed carbon structures without CNWs (no plasma treatment, Figure 5G and SI) illustrate that the CNW structures exhibit significantly greater DNA binding. The fluorescence intensity increased by 750% from 31 au to 234 au by nanostructuring, which is also higher than our previous experiments performed on graphene-like flakes, which obtained *ca.* 60 au.³⁶ Bleaching experiments clearly showed that the fluorescence is originating from the labeled DNA and not the underlying carbon. During

the above experiments the carbon nanostructures are repeatedly immersed and rinsed in various liquids (see SI). Forces arising during this procedure can damage the samples, and improving the robustness of the structures is therefore an important aspect of ongoing research.

Finally, DNA binding was detected electrically by a four-probe resistance measurement of functionalized 3D bridge structures. Measurements were repeated several times on amorphous carbon bridges both with and without CNWs. In each case, we compared a positive sample, where DNA was covalently bonded to the carbon, and a negative sample, where DNA was added to the solution but not bonded to the carbon (no EDC cross-linker added). The resistance of the DNA-coupled CNW arches was 40% lower than the negative samples (Figure 5H). This drop in resistance is likely due to the DNA-induced charge transfer,⁶ which improves electrical transport through the arch structure. However, no resistance change was measured for the structures without CNWs, as shown in Figure 5H. Because Raman (Figure 1E) and XPS data (Table S1) suggest both structure have a similar material composition, the changes in sensitivity are attributed to the CNWs. Through further

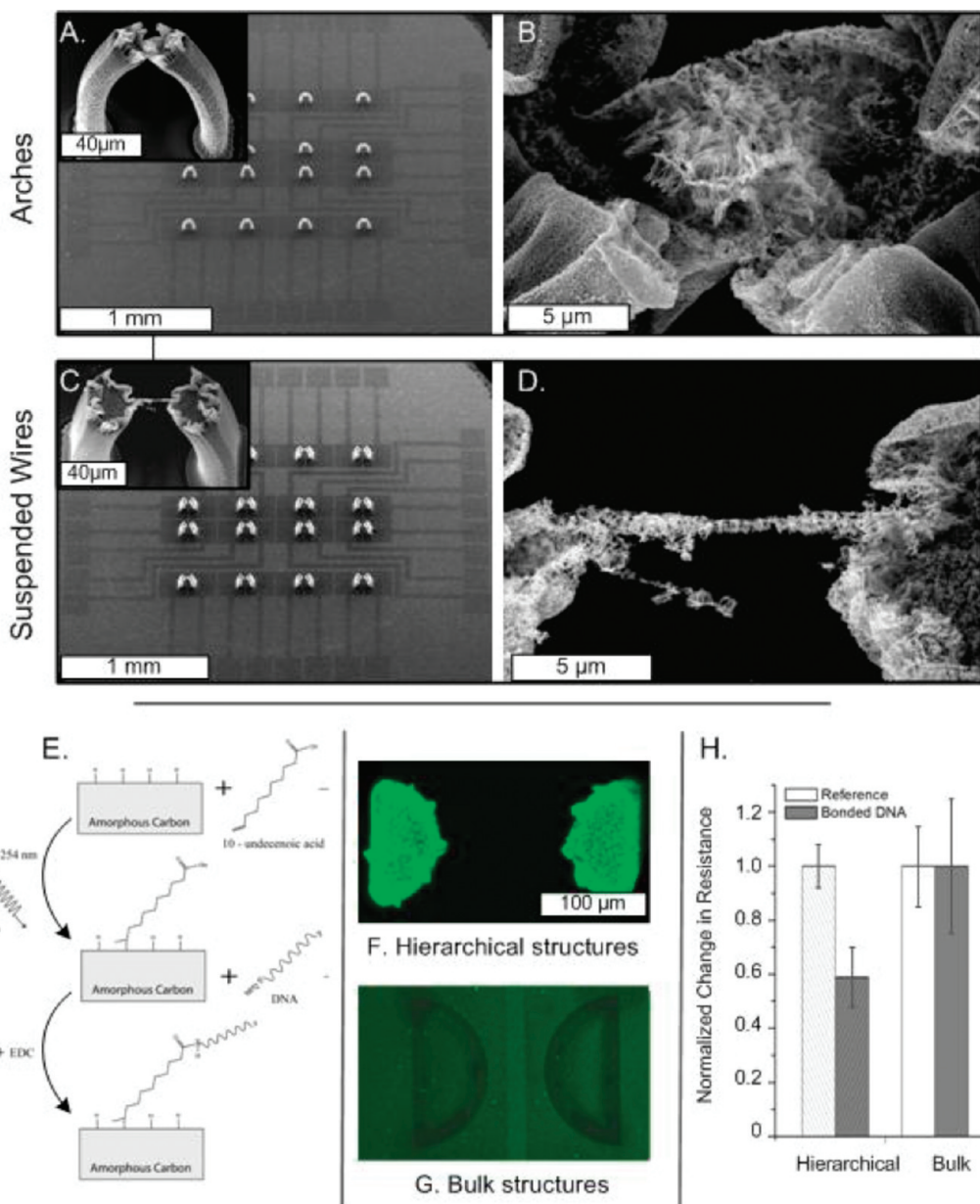


Figure 5. CNW arch sensor arrays fabricated on TiN bottom electrodes and their application to DNA binding detection. (A, B) SEM images of arch-shaped sensing node arrays. (C, D) SEM images of suspended-wire sensing node arrays. (E) Scheme for covalent binding of a DNA strand to CNW microstructures. (F, G) Fluorescence microscopy of bulk pyrolyzed SU8 and hierarchically nanostructured micropillars after DNA binding. (H) Change in resistance of CNW arch sensors after binding of DNA, compared to identical structure made by pyrolysis of SU8 without plasma etching. The average resistance of the negative reference samples is normalized to 1.

study of the binding kinetics and DNA hybridization, these CNW sensors could be integrated in disposable lab-on-chip systems for point of care applications.

CONCLUSIONS

In closing, we presented a new method for hierarchical nanostructuring of carbon into novel microarchitectures of aligned carbon nanowires. This method is scalable and highly versatile and requires only standard lithography, oxygen plasma treatment, and thermal processing. This method therefore complements both the morphology and fabrication methods of existing

nanostructured carbon.^{38,39} Preliminary experiments show that electrically integrated CNW forests could greatly increase the sensitivity of biosensors, and we envision that this may also be true for other systems requiring electrochemically stable electrodes with a large surface area such as batteries,⁴⁰ fuel cells,⁸ and biochemical probes.²²

Acknowledgment. This work was supported by the Fund for Scientific Research, Flanders, Belgium (FWO), and the IAP VI/42. The authors thank D. Cott for help with the Raman spectroscopy, and T. Conard for XPS measurements. Furthermore, we thank Dr. A. Ethirajan and Prof. M. Ameloot for sci-

entific advice and access to the fluorescence microscopy facilities.

Supporting Information Available: Detailed XPS measurements of the developed material at different stages of the fabrication process; examples of bulk pyrolyzed sensor arrays based on microarches; and detailed information of the biosensor chemistry used during our experiments. This material is available free of charge via the Internet at <http://pubs.acs.org>.

REFERENCES AND NOTES

- Schueller, O. J. A.; Brittain, S. T.; Whitesides, G. M. Fabrication of Glassy Carbon Microstructures by Soft Lithography. *Sensors Actuators, A* **1999**, *72*, 125–139.
- Wang, C. L.; Jia, G. Y.; Taherabadi, L. H.; Madou, M. J. A Novel Method for the Fabrication of High-Aspect Ratio C-MEMS Structures. *J. Microelectromech. Syst.* **2005**, *14*, 348–358.
- Jaramillo, M. D.; Torrents, E.; Martinez-Duarte, R.; Madou, M. J.; Juarez, A. On-Line Separation of Bacterial Cells by Carbon-Electrode Dielectrophoresis. *Electrophoresis* **2010**, *31*, 2921–2928.
- Du, R. B.; Ssenyange, S.; Aktary, M.; McDermott, M. T. Fabrication and Characterization of Graphitic Carbon Nanostructures with Controllable Size, Shape, and Position. *Small* **2009**, *5*, 1162–1168.
- Martinez-Duarte, R.; Gorkin, R. A.; Abi-Samra, K.; Madou, M. J. The Integration of 3D Carbon-Electrode Dielectrophoresis on a CD-Like Centrifugal Microfluidic Platform. *Lab Chip* **2010**, *10*, 1030–1043.
- Davis, F.; Hughes, M. A.; Cossins, A. R.; Higson, S. P. J. Single Gene Differentiation by DNA-Modified Carbon Electrodes Using an AC Impedimetric Approach. *Anal. Chem.* **2007**, *79*, 1153–1157.
- Sun, B.; Colavita, P.; Kim, H.; Lockett, M.; Marcus, M.; Smith, L.; Hamers, R. Covalent Photochemical Functionalization of Amorphous Carbon Thin Films for Integrated Real-Time Biosensing. *Langmuir* **2006**, *22*, 9598–9605.
- Lin, P. C.; Park, B. Y.; Madou, M. J. Development and Characterization of a Miniature PEM Fuel Cell Stack with Carbon Bipolar Plates. *J. Power Sources* **2008**, *176*, 207–214.
- Yun, W.; Pham, L.; de Vasconcellos, G. P. S.; Madou, M. Fabrication and Characterization of Micro PEM Fuel Cells Using Pyrolyzed Carbon Current Collector Plates. *J. Power Sources* **2010**, *195*, 4796–4803.
- Teixidor, G. T. G. Turon; Gorkin, R. A.; Tripathi, P. P.; Bisht, G. S.; Kulkarni, M.; Maiti, T. K.; Bhattacharyya, T. K.; Subramanian, J. R.; Sharma, A.; Park, B. Y.; et al. Carbon Microelectromechanical Systems as a Substratum for Cell Growth. *Biomed. Mater.* **2008**, *3*.
- Steach, J. K.; Clark, J. E.; Olesik, S. V. Optimization of Electrospinning an SU-8 Negative Photoresist to Create Patterned Carbon Nanofibers and Nanobeads. *J. Appl. Polym. Sci.* **2010**, *118*, 405–412.
- Sharma, C. S.; Sharma, A.; Madou, M. Multiscale Carbon Structures Fabricated by Direct Micropatterning of Electrospun Mats of SU-8 Photoresist Nanofibers. *Langmuir* **2001**, *17*, 2218–2222.
- Penmatsa, V.; Yang, J. H.; Yu, Y.; Wang, C. L. Fabrication of Porous Carbon Micropillars Using a Block Copolymer as Porogen. *Carbon* **2010**, *48*, 4109–4115.
- Sharma, C. S.; Katepalli, H.; Sharma, A.; Madou, M. Fabrication and Electrical Conductivity of Suspended Carbon Nanofiber Arrays. *Carbon* **2011**, *49*, 1727–1732.
- Tang, Y. H.; Wang, N.; Zhang, Y. F.; Lee, C. S.; Bello, I.; Lee, S. T. Synthesis and Characterization of Amorphous Carbon Nanowires. *Appl. Phys. Lett.* **1999**, *75*, 2921–2923.
- Sanchez, C.; Arribart, H.; Guille, M. M. G. Biomimetic and Bioinspiration as Tools for the Design of Innovative Materials and Systems. *Nat. Mater.* **2005**, *4*, 277–288.
- Daccord, G.; Lenormand, R. Fractal Patterns from Chemical Dissolution. *Nature* **1987**, *325*, 41–43.
- Huang, J. H.; Kim, J.; Agrawal, N.; Sudarson, A. P.; Maxim, J. E.; Jayaraman, A.; Ugaz, V. M. Rapid Fabrication of Bio-inspired 3D Microfluidic Vascular Networks. *Adv. Mater.* **2009**, *21*, 3567.
- Kharissova, O. V.; Kharisov, B. I. Less-Common Nanostructures in the Forms of Vegetation. *Ind. Eng. Chem. Res.* **2010**, *49*, 11142–11169.
- Soleymani, L.; Fang, Z. C.; Sargent, E. H.; Kelley, S. O. Programming the Detection Limits of Biosensors through Controlled Nanostructuring. *Nat. Nanotechnol.* **2009**, *4*, 844–848.
- Soleymani, L.; Fang, Z. C.; Sun, X. P.; Yang, H.; Taft, B. J.; Sargent, E. H.; Kelley, S. O. Nanostructuring of Patterned Microelectrodes To Enhance the Sensitivity of Electrochemical Nucleic Acids Detection. *Angew. Chem., Int. Ed.* **2009**, *48*, 8457–8460.
- Nguyen-Vu, T. D. B.; Chen, H.; Cassell, A. M.; Andrews, R.; Meyyappan, M.; Li, J. Vertically Aligned Carbon Nanofiber Arrays: An Advance toward Electrical-Neural Interfaces. *Small* **2006**, *2*, 89–94.
- Boesel, L. F.; Greiner, C.; Arzt, E.; del Campo, A. Gecko-Inspired Surfaces: A Path to Strong and Reversible Dry Adhesives. *Adv. Mater.* **2010**, *22*, 2125–2137.
- Gao, H. J.; Wang, X.; Yao, H. M.; Gorb, S.; Arzt, E. Mechanics of Hierarchical Adhesion Structures of Geckos. *Mech. Mater.* **2005**, *37*, 275–285.
- Walther, F.; Davydovskaya, P.; zucher, S.; Kaiser, M.; Herberg, H.; Gigler, A. M.; Stark, R. W. Stability of the Hydrophilic Behavior of Oxygen Plasma Activated SU-8. *J. Micromech. Microeng.* **2007**, *17*, 524–531.
- Tsougeni, K.; Vourdas, N.; Tserepi, A.; Gogolides, E.; Cardinaud, C. Mechanisms of Oxygen Plasma Nanotexturing of Organic Polymer Surfaces: From Stable Super Hydrophilic to Super Hydrophobic Surfaces. *Langmuir* **2009**, *25*, 11748–11759.
- Wang, C. L.; Zaouk, R.; Madou, M. Local Chemical Vapor Deposition of Carbon Nanofibers from Photoresist. *Carbon* **2006**, *44*, 3073–3077.
- Teshima, K.; Sugimura, H.; Inoue, Y.; Takai, O.; Takano, A. Transparent Ultra Water-Repellent Poly(ethylene Terephthalate) Substrates Fabricated by Oxygen Plasma Treatment and Subsequent Hydrophobic Coating. *Appl. Surf. Sci.* **2005**, *244*, 619–622.
- Schueller, O. J. A.; Brittain, S. T.; Whitesides, G. M. Fabrication of Glassy Carbon Microstructures by Pyrolysis of Microfabricated Polymeric Precursors. *Adv. Mater.* **1997**, *9*, 477.
- Hata, K.; Futaba, D. N.; Mizuno, K.; Namai, T.; Yumura, M.; Iijima, S. Water-Assisted Highly Efficient Synthesis of Impurity-Free Single-Walled Carbon Nanotubes. *Science* **2004**, *306*, 1362–1364.
- Copic, D.; Park, S. J.; Tawfick, S.; De Volder, M. F. L.; Hart, A. J. Fabrication of High-Aspect-Ratio Polymer Microstructures and Hierarchical Textures using Carbon Nanotube Composite Master Molds. *Lab Chip* **2011**, *11*, 1831–1837.
- Baughman, R. H.; Zakhidov, A. A.; de Heer, W. A. Carbon Nanotubes - the Route Toward Applications. *Science* **2002**, *297*, 787–792.
- Brooksby, P. A.; Downard, A. J. Nanoscale Patterning of Flat Carbon Surfaces by Scanning Probe Lithography and Electrochemistry. *Langmuir* **2005**, *21*, 1672–1675.
- Lee, J. A.; Lee, S.; Lee, K. C.; Il Park, S.; Lee, S. S. Fabrication and Characterization of Freestanding 3D Carbon Microstructures using Multi-Exposures and Resist Pyrolysis. *J. Micromech. Microeng.* **2008**, *18*.
- Lee, S. J.; Shi, W.; Maciel, P.; Cha, S. W. Top-Edge Profile Control for SU-8 Structural Photoresist. Proceedings of the 15th Biennial University/Government/Industry Microelectronics Symposium (Cat. No. 03CH37488). **2003**, 389–90|397.
- Vanswevel, R.; Malesevic, A.; Van Gompel, M.; Vanhulsel, A.; Wenmackers, S.; D'Haen, J.; Vermeeren, V.; Ameloot, M.; Michiels, L.; Van Haesendonck, C.; et al. Biological Modification of Carbon Nanowalls with DNA Strands and Hybridization Experiments with Complementary and Mismatched DNA. *Chem. Phys. Lett.* **2010**, *485*, 196–201.
- Christiaens, P.; Vermeeren, V.; Wenmackers, S.; Daenen, M.; Haenen, K.; Nesladek, M.; vandeVen, M.; Ameloot, M.;

- Michiels, L.; Wagner, P. EDC-Mediated DNA Attachment to Nanocrystalline CVD Diamond Films. *Biosens. Bioelectron.* **2006**, 22, 170–177.
38. De Volder, M.; Tawfick, S. H.; Park, S. J.; Copic, D.; Zhao, Z. Z.; Lu, W.; Hart, A. J. Diverse 3D Microarchitectures Made by Capillary Forming of Carbon Nanotubes. *Adv. Mater.* **2010**, 22, 4384–4389.
39. Hayamizu, Y.; Yamada, T.; Mizuno, K.; Davis, R.; Futaba, D.; Yumura, M.; Hata, K. Integrated Three-Dimensional Microelectromechanical Devices from Processable Carbon Nanotube Wafers. *Nat. Nanotechnol.* **2008**, 3, 289–294.
40. Hong-Seok, M.; Park, B. Y.; Taherabadi, L.; Wang, C.; Yeh, Y.; Zaouk, R.; Madou, M. J.; Dunn, B. Fabrication and Properties of a Carbon/Polypyrrole Three-Dimensional Micrbattery. *J. Power Sources* **2008**, 178, 795–800.